CrossMark

ORIGINAL PAPER

Superconducting Properties of $FeSe_{0.5}Te_{0.5}$ Under High Pressure

Esmeralda Martínez-Piñeiro[1] · Roberto Escudero[1]

Abstract This work reports studies performed in the superconducting compound $FeSe_{0.5}Te_{0.5}$ under high pressure. Changes were observed in the transition temperature, superconducting critical fields, anomalous variations in the Meissner fraction, and in Ginzburg Landau parameters. The superconducting properties were calculated and compared using the Werthamer-Helfand-Hohenber approximation and Ginzburg-Landau theory. Hydrostatic pressure was produced from atmospheric to 823 MPa, the increment in the critical temperature was from 14.45 to 20.5 K at a rate of change about 0.0069 K/MPa.

Keywords Superconductivity · FeSe · Magnetism · High pressure

1 Introduction

The recent discovery of the Fe-based superconductors has proved that superconductivity and ferromagnetism may coexists with the consequent changes on the electronic pair formation, different to the electron-phonon type described by the BCS theory [1]. The new type of superconducting materials opens other possibilities for the electron pairing and the perspectives to explore different processes on superconducting compounds with magnetic elements, for instances the recent results by Nakayama et al. in $FeSe$ film with K doping, discovered that the cross-interfacial electron-phonon coupling was not the primary interaction for the superconducting pairing [2, 3]. The superconducting family of compounds with Fe and chalcogenides, i.e., $Fe(Se, Te)$ has a simple crystal structure known as the anti-PbO, with $P4/mmm$ symmetry [4]. Physical modifications on these structures, particularly on the Fe-Se bonds, give place to other superconducting compounds with different transition temperatures [5]. Yeh et al. have investigated that the transition temperature in these compounds changes because the coupling between layers can be modified via chemical and/or external pressures [6–9]. One example of these changes was observed in the $FeSe$ [10] where the transition temperature T_C changes with the internal pressure when selenium is substituted by tellurium resulting the family of $FeSe_{1-x}Te_x$. In the particular case of $FeSe_{0.5}Te_{0.5}$, the internal pressure increases the T_C from 8 to 15 K [11]. Moreover, other manner to produce changes in the electronic and structural properties on these compounds is by applying high pressures by external means. The tools to produce external pressures are called pressure cells. The most powerful of these instruments are the diamond pressure cells that are able to produce pressures of the order of hundred of GPa at hydrostatic or quasi-hydrostatics forms. Here, in this work, we used a pressure cell without diamonds that is able to produce in a simple manner hydrostatic pressures at the order of a few MPa. So, this cell was used to investigate the range not yet studied of the variations of critical fields and Ginzburg-Landau parameters at pressures of only a few MPa.

Recent pressure studies of the $Fe(Se, Te)$ family were focused in the observation of changes on T_C and in its crystal structure. In a report by Stemshorn et al. [12], the authors indicate that the $FeSe$ tetragonal structure ($P4/nmm$) was transformed to an hexagonal one ($P6_3/mmc$) with applied

✉ Roberto Escudero
escu@unam.mx

[1] Instituto de Investigaciones en Materiales, Universidad Nacional Autónoma de México, A. Postal 70-360, México, DF, 04510 México

pressure and becoming amorphous at higher pressures. On the other hand, it was observed that $FeSe_{0.5}Te_{0.5}$ increased its T_C to 26 K at $P = 2$ GPa while higher pressures produces structural transitions to a monoclinic symmetry that decreases T_C [13–15]. Moreover at $P = 11.5$ GPa, the compound changes into an amorphous phase [16, 17]. In a recent report Pietosa et al. studied the pressure effects on the critical fields up to 1.04 GPa founding no important variations on the behavior of the dH_{C2}/dT, concluding that the observed changes on the upper critical field was related only to changes of T_C [18].

In this work, we investigated the behavior and changes on the critical fields of $FeSe_{0.5}Te_{0.5}$ under hydrostatic pressures below 900 MPa. Our investigation pointed out that this behavior is almost independent of the variations of T_C. The primary objective of this research is to study the behavior on the critical fields, Ginzburg-Landau parameters and thermodynamic properties at different pressures. It is important to mention that this superconductor has been scarcely studied under the influence of external pressures below 1 GPa. Other researchers have attributed those changes to variations on the density of the superconducting carriers. However, that analyses by Fedor et al. was not very conclusive, and the main part of their investigations was mainly focused to observe the T_C variations instead on the behavior superconducting properties [19].

2 Experimental Details

$FeSe_{0.5}Te_{0.5}$ samples were prepared by solid state reactions starting with stoichiometric amounts of selenium powder (Alfa Aesar, 99.99 %), tellurium powder (Alfa Aesar, 99.999 %), and iron pieces (Merck, 99.999 %) and were mixed and powdered in an agatha mortar and pelletized. The resulting samples were vacuum-sealed in quartz tubes and heated at 1000 °C during 40 h. After this, the procedure was cooled at a rate of 10 °C/h following the similar procedure as already published [20, 21]. Crystal structural analysis was performed by X-ray diffraction and scanning electron microscopy. X-ray studies were obtained using a D5000-Siemens diffractometer with $Co - K\alpha$ radiation. Compositions of the samples were estimated using a field emission scanning electron microscopy (JEOL JSM 7600F) coupled with energy dispersive x-ray spectroscopy (EDX, Oxford). Superconducting properties were determined by magnetic measurements with a SQUID-based magnetometer (Quantum Design MPMS). High pressure measurements were performed with a CuBe cell (Quantum Design) using a small piece of Pb as the manometer, for the pressure media was used Daphne 7373 oil. In order to subtract the magnetic background, the cell was measured without sample [22]. Daphne pressure oil medium was used because

of its lack of magnetic contribution when the temperature decreases [23]. The superconducting transition temperatures were determined by magnetic susceptibility with field of 20 Oe oriented parallel to the ab-plane in two modes, zero field cooling ZFC, and field cooling FC.

3 Results and Discussion

Diffraction analysis determined that the compound has $FeSe_{0.44}Te_{0.56}$ with very small traces of $\beta - FeSe$, as shown in Fig. 1. The compound presents anti-PbO crystalline structure and $P4/nmm$ symmetry (CSD 421334) [24] with preferential orientation on the plane [100], the non superconducting compound $\beta - FeSe$ has NiAs-type structure and $P6_3/mmc$ symmetry (ICDD 85-0735) [25].

A small sample was studied with SEM, it shows lamellar structure, see Fig. 1 inset, confirming that the compound was highly oriented. Backscattered electron images reveal regions of light gray homogeneous coloration corresponding to richer parts of Te as already explained by Pimentel et al. [26], while dark zones are produced by the surface morphology. EDX analysis was used to determine that averaged composition was $Fe_{1.09}Se_{0.45}Te_{0.55}$, results were consistent with SEM images and DRX analysis.

Superconducting properties of $Fe_{1.09}Se_{0.45}Te_{0.55}$ were studied at low temperatures and ambient pressure with DC Magnetic susceptibility, $\chi(T)$. Those measurements are presented in Fig. 2. The inset shows a plot from 2 o 30 K. Demagnetization factor was estimated to be 0.826 due to the shape and size of the sample [27, 28]. Figure 2 also shows a small paramagnetic contribution due to $\beta - FeSe$, this
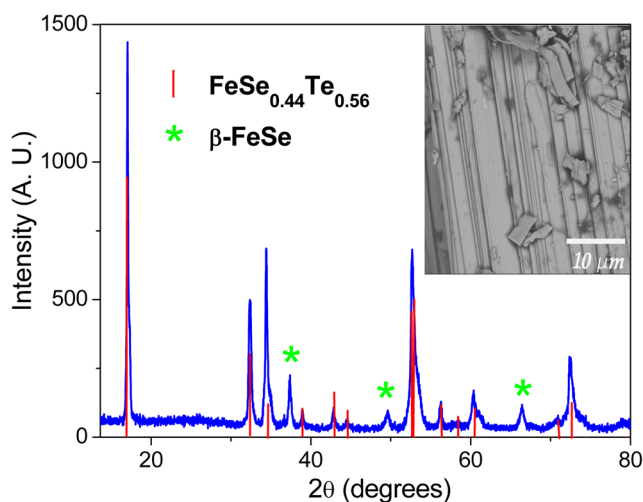

Fig. 1 (*Color online*) Diffraction patterns of sample, $FeSe_{0.44}Te_{0.56}$ with small traces of the non-superconducting FeSe Achavalite structure, those reflections are signaled with ∗. The inset shows SEM images of backscattering electrons and the homogeneous layered sample
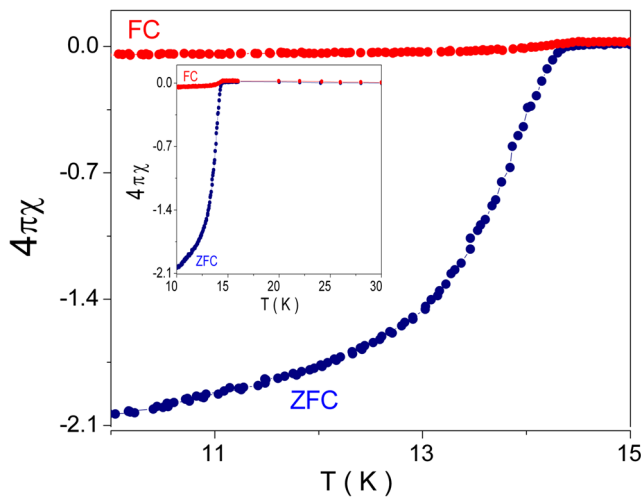
Fig. 2 (*Color online*) Transition temperature, $T_C = 14$ K of the compound $FeSe_{0.44}Te_{0.56}$ measured in FC and ZFC modes. The inset shows the temperature dependence of the DC magnetic susceptibility at low temperatures

is seen above the superconducting transition in the inset. There, also is shown the ZFC mode which is about 50 times bigger than the FC mode. It is important to mention that this behavior has been attributed to strong pinning effects as in [29].

Once the sample was characterized at room atmospheric pressure, high pressure measurements were performed with the sample inside of the CuBe cell. DC magnetic measurements were performed into two modes under different hydrostatic pressures. The results of these measurements are illustrated in Fig. 3, measurements are displayed in terms of $4\pi\chi$ units.

The transition temperature was taken when $\chi(T)$ curve deviates from the zero background value. The results show
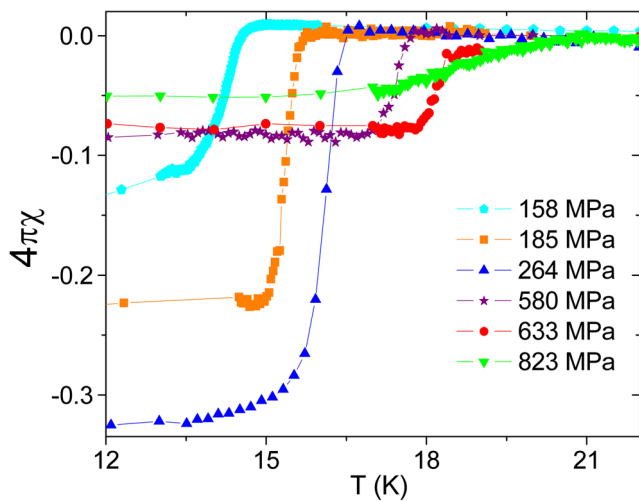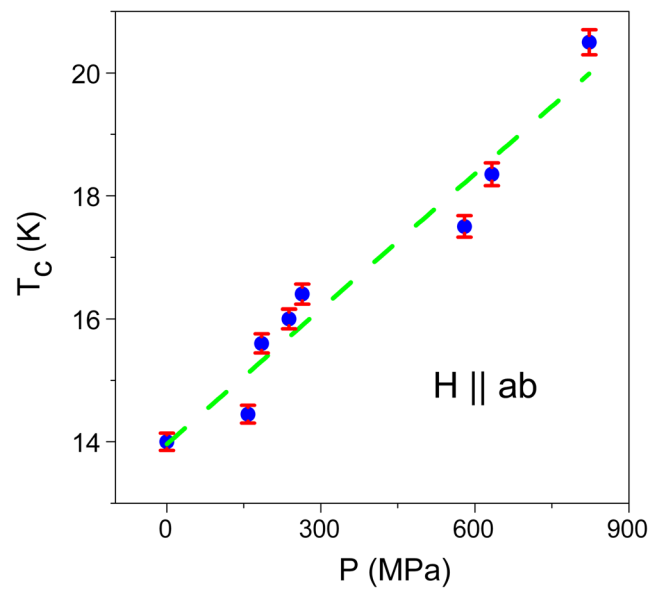

Fig. 4 (*Color online*) Changes experimented by the transition temperature with pressure, $T_C - P$. The rate of change is linear and varies as 0.0069 K/MPa similar to other measurements

that T_C increases continuously with the pressure. Figure 4 shows a plot of the changes experimented of the T_C by pressure effects with the linear fit of $T_C - P$ extracted from Fig. 3.

The Meissner fraction was calculated with $-4\pi\chi = -4\pi\rho M/mB$, where ρ is the sample density, equal to 6.06 g/cm^3, M is the magnetization, m is the mass of the sample, and B is the applied magnetic field [30]. Figure 5 shows the Meissner fraction determined at different pressures. The Meissner fraction increases with pressure from 13 % at a $P = 158$ MPa to about 34 % at $P = 264$ MPa. With higher pressures, about $P = 580$ MPa, the fraction
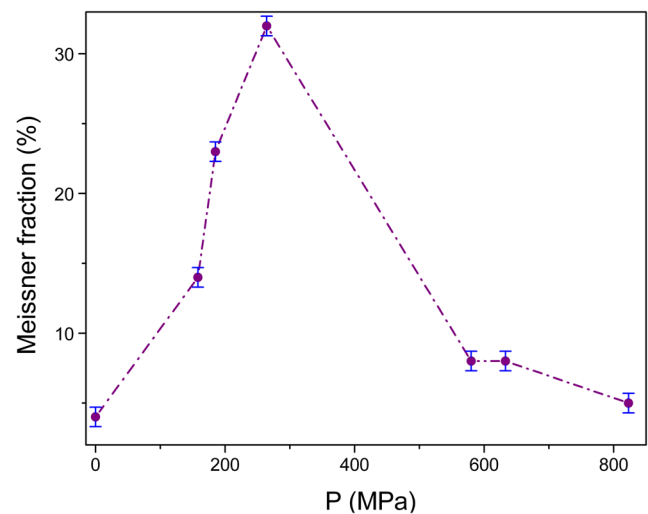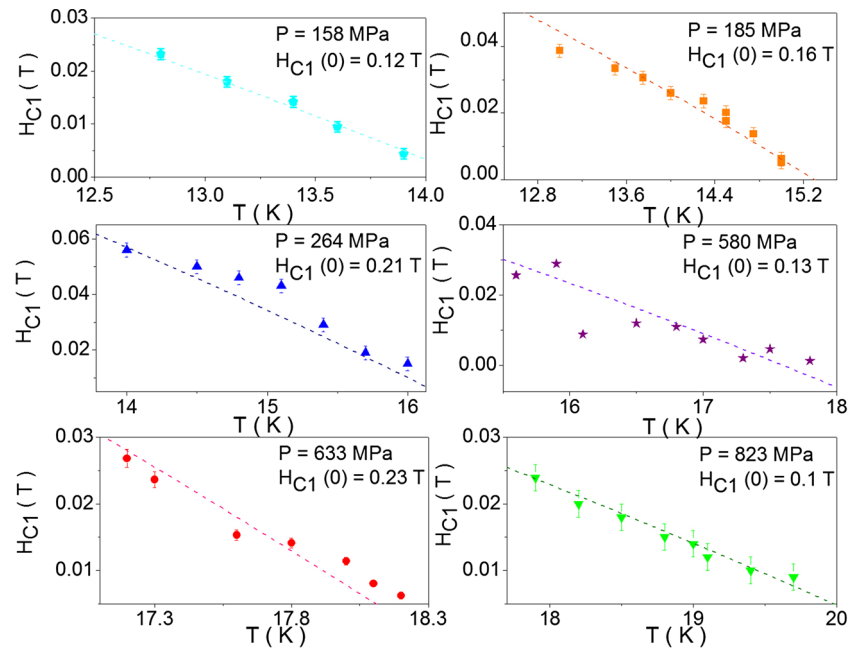

Fig. 3 (*Color online*) Field cooling measurements near T_C at different pressures

Fig. 5 (*Color online*) Meissner fraction changes with pressure in the $Fe_{1.09}Se_{0.45}Te_{0.55}$ sample

Fig. 6 (*Color online*) Lower critical field, $H_{C1}(0)$ versus applied pressure estimated with the formula described in the text

decreases at about 8 %. We have to note that an anomalous increase is observed at 264 MPa, the fraction is highly increased, and with increasing pressure, it decreases dramatically. In other studies in $BaFe_2(As_{1-x}P_x)_2$ [31] and $La_{2-x}Sr_xCuO_4$ [32], it was observed a similar behavior in experiments with substituting atoms and producing internal pressures. Those similar experiments demonstrate that the Meissner fraction could varies in a non-monotonic way with the pressure. However, we believe that more experimental work will be necessary in order to investigate more about this behavior. Lastly, it is very important to mention that in most of the literature never was studied or observed the Meissner fraction changes because the signals were very small and the FC and ZFC measurements have an enormous differences between them.

Critical magnetic field measurements were performed and determined with isothermal magnetization curves. For determinations of the lower critical fields, H_{C1} we used in those curves the point where the diamagnetic curve start to deviate from linearity. $H_{C1}(T)$ temperature dependence was

fitted with equation: $H_{C1}(T) = H_{C1}(0)(1 - (T/T_C)^2)$, as shown in Fig. 6 and in Table 1.

The upper critical field H_{C2} was calculated with the linear fit from experimental data near T_C and using the Werthamer-Helfand-Hohenberg (WHH) approximation [33]. This approximation is given by; $H_{C2}(0) = -0.693 T_C \frac{dH_{C2}(T)}{dT}|_{T=T_C}$, where $\frac{dH_{C2}(T)}{dT}|_{T=T_C}$ corresponds to the slope of the linear fit. The Ginzburg-Landau parameters, coherence length ξ_{GL}, penetration length λ_{GL}, κ, and the thermodynamic critical field $H_C(0)$ were estimated with the equations: $H_{C2}(0) = \phi_0/2\pi\xi_{GL}^2$, $H_{C2}(0)/H_{C1}(0) = 2\kappa^2/\ln\kappa$, $\kappa = \lambda_{GL}/\xi_{GL}$, $H_C(0) = \phi_0/(2\sqrt{2}\pi\xi_{GL}\lambda_{GL})$, where ϕ_0 is the quantum magnetic flux.

In this analysis, the upper critical field shows a concave upward feature near T_C, see illustration in Fig. 7. This behavior is attributed to multiband response and has been also observed in other iron-selenides compounds by Jing et al. and Bezusyy et al. [34, 35] and in $Na_{0.35}CoO_2 yH_2O$ by Kao et al. [36]. For our calculations of the critical fields, we use a linear fit excluding the curve zone, as it was

Table 1 Superconducting parameters

P (MPa)	T_C (K)	$H_{C1}(0)$ (T)	$-dH_{C2}/dT$ (T/K)	$H_{C2}(0)$ (T)	ξ_{GL} (nm)	κ	$H_C(0)$ (T)	λ_{GL} (nm)
0	14.5	0.03(0)	0.15(3)	1.50(7)	1.4(7)	6.9(5)	0.15(2)	102.69(7)
158	14.7	0.12(2)	0.91(2)	9.16(8)	5.9(9)	9.2(0)	0.70(3)	55.1(2)
185	15.6	0.16(0)	2.10(2)	22.72(4)	3.8(1)	13.6(1)	1.18(1)	51.7(5)
264	16.4	0.21(3)	1.65(9)	18.85(7)	4.1(8)	10.2(90)	1.30(4)	42.6(1)
580	17.5	0.13(4)	2.92(1)	35.428(4)	3.0(5)	19.6(1)	1.25(7)	59.7(4)
633	18.4	0.23(3)	1.40(2)	17.80(3)	4.2(9)	9.2(5)	1.35(2)	39.7(7)
823	20.5	0.10(1)	0.97(0)	13.78(0)	4.8(8)	13.3(1)	0.72(7)	65.0(5)

Fig. 7 (*Color online*) Upper critical fields versus temperature determined with the WHH approximation
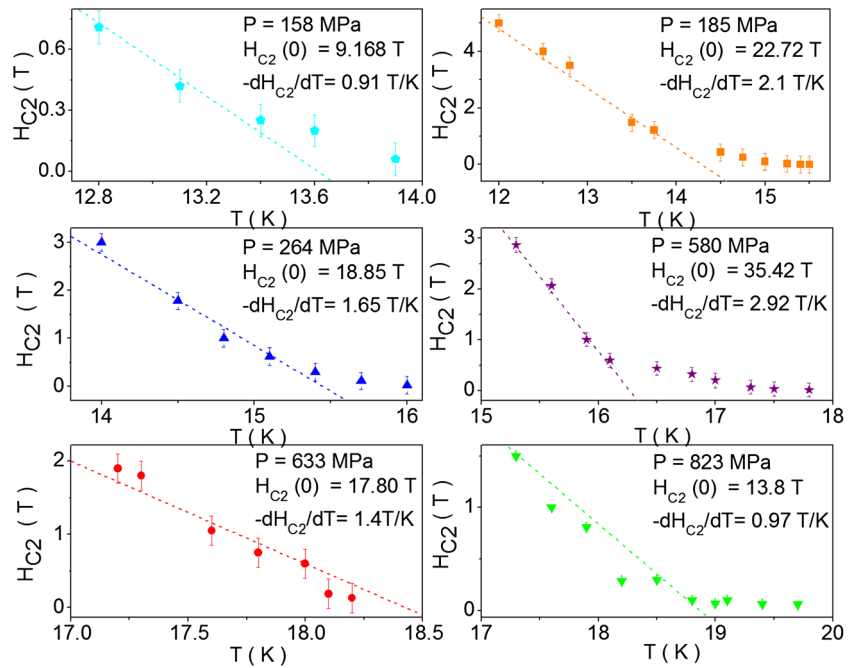
performed by Pietosa. Note that the slope $-dH_C/dT$ has different values for each pressure. In some investigations [18], the authors have considered that the increment on the critical fields is caused only by the increment of T_C. Our experiments clearly indicate that the critical fields reach the highest value at $P = 600$ MPa, instead of 823 MPa, these values are shown in Fig. 8. In order to assure that this behavior is correct, our measurements were repeated at least twice using different samples.

With the help of Ginzburg-Landau theory, the superconducting parameters were determined and shown in Table 1.
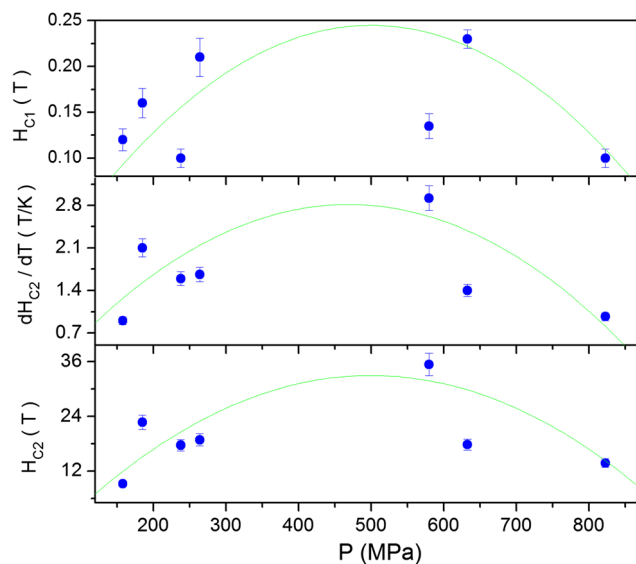

Fig. 8 (*Color online*) Critical fields versus pressure

Those parameters are similar to the data measured at normal ambient pressure [11, 20, 21]. We found that some parameters vary in irregular form and present anomalous values. λ_{GL} for instances decreases more than 50 % as pressure is applied and then shows a small increment at higher pressure. This may implies a considerable increment on the superconducting electronic density. Coherence length also is increased by about 400 % at $P = 158$ MPa. According to our experiments, and others, pressure strongly affect the superconducting parameters and these changes can be attributed not only to increment of T_C but to additional factors, as crystal parameters and structural changes, etc [17]. In our investigation, we noticed that the T_C, critical fields, and superconducting parameter are very sensitive to pressure, being a clear sign that this compound presents unconventional superconductivity [37].

4 Conclusions

Magnetic studies under hydrostatic pressure were performed in $FeSe_{0.5}Te_{0.5}$ in order to investigate the impact of pressure on the basic parameters of this superconductor. We found a linear increase of T_C that changes from 14.03 to 20.5 K, at a rate of 0.0069 K/MPa. The anomalous behavior of the Meissner fraction and superconducting parameters is difficult to explain because those are not directly related to changes of the transition temperature with pressure. As mentioner earlier, the changes in pressure may be associated with $Se-Fe-Se$ interlayer separation [38]. On the other hand, the dependence of superconducting properties

with pressure of this compound implying that microscopic mechanism of the electronic pairing is different of electron-phonon, as it is shown in unconventional superconductors. Other reports on similar studies [39, 40] indicate that the increment of the density of electronic states are not enough to the explanation of the notable increment of the transition temperature. The presence of a Peierls distortion, as a Spin Density Wave, must be decreased by pressure but nevertheless has any influence on the transition temperature, again this is quite anomalous. Lastly, we must mention that still more experiments are necessary in order to completely understand this type of new superconducting materials [41, 42].

References

1. Kordyuk, A.A.: Low Temp. Phys. **38**, 888 (2012)
2. Miyata, Y., et al.: Nat. Mater. **14**, 285 (2015)
3. Mazin, I.: Nat. Mater. **14**, 755 (2015)
4. Yeh, K.W., et al.: J. Phys. Soc. Jpn. **77**, 152505 (2008)
5. Yeh, K.W., et al.: Eur. Phys. Lett. **84**, 37002 (2008)
6. Fong-Chi, H., et al.: PNAS 105 **38**, 14262 (2008)
7. Stemshorn, A., et al.: High Press. Res. **29**, 267 (2009)
8. Yoshikazu, M., et al.: Physica C **470**, 5353 (2010)
9. Mizuguchi, et al.: Physica C **470**, S353–S355 (2010)
10. Sales, B.C., et al.: Phys. Rev. B **79**, 094521 (2009)
11. Horigane, K., et al.: J. Phys. Soc. Jpn. **78**(40143431), 074718 (2009)
12. Stemshorn, A.K., et al.: J. Mater. Res. **25**, 396 (2010)
13. Horigane, K., et al.: J. Phys. Soc. Jpn. **78**(40143095), 063705 (2009)
14. Tsoi, G., et al.: J. Phys. Condens. Matter **21**, 232201 (2009)
15. Huang, Ch.-L., et al.: J. Phys. Soc. Jpn. **78**, 084710 (2009)
16. Gresty, N.C., et al.: J. Am. Chem. Soc. **131**, 16944 (2009)
17. Pallavi, M., et al.: 125701 **26**(12) (2014)
18. Pietosa, J., et al.: J. Phys. Condens. Matter **24**, 265701 (2012)
19. Fedorchenko, A.V., et al.: Low Temp. Phys. **37**, 83 (2011)
20. Velasco-Soto, D., et al.: J. Appl. Phys. **113**, 7E138 (2013)
21. Awana.: J. Appl. Phys. **107**, 09E128 (2010)
22. Quantum Design, CuBe Cell manual, (2010)
23. Kamard, J., et al.: Rev. Sci. Instrum. **75**, 5022 (2004)
24. Tegel, M., et al.: Solid State Commun. **150**, 383–385 (2010)
25. Gomez, R.W., et al.: J. Supercond. Novel Magn. **23**, 551 (2010)
26. Pimentel, J., et al.: J. Appl. Phys. **111**, 033908 (2012)
27. Amikam, A.: J. Appl. Phys. **83**, 3432 (1998)
28. Dajerowsky, D., et al.: New J. Chem. **35**, 1320 (2011)
29. Bendele, et al.: Phys. Rev. B **81**, 224520 (2010)
30. Lai, C., et al.: Physica C **470**, 313 (2010)
31. Jiang, S., et al.: J. Phys. Condens. Technol. **16**, l7–L9 (2003)
32. Zhou, F., et al.: Super. Cond. Sci. Matter **21**(38), 382203 (2009)
33. Li, L.F., et al.: Physica C **470**, 313 (2010)
34. Zhang, J.-L., et al.: Front. Phys. **6**, 4 (2011)
35. Bezusyy, V.L., et al.: Acta Polonica series A **121**(4), 816 (2012)
36. Kao, J., et al.: Phys. Rev. B **75**(1), 012503 (2007)
37. Mineev, V.P., Samokhin, K.V.: Introduction to unconventional superconductivity. Gordon and Breach, London (1999)
38. Margadonna, et al.: Phys. Rev. B **80**, 064506 (2009)
39. Lu, H., et al.: J. Low Temp. Phys. **178**, 355 (2015)
40. Ciechan, A., et al.: Acta Physica Polonica A **121**(4), 821 (2012)
41. Koufos, A., Papaconstantopoulos, D.: Phys. Rev. B **89**, 035150 (2014)
42. Mandal, S., et al.: Phys. Rev. B **89**, 220502(R) (2014)